AMERICAN SOCIETY FOR MICROBIOLOGY | mBio®

RESEARCH ARTICLE

YhdP, TamB, and YdbH Are Redundant but Essential for Growth and Lipid Homeostasis of the Gram-Negative Outer Membrane

Natividad Ruiz,[a] Rebecca M. Davis,[a] Sujeet Kumar[a]

[a]Department of Microbiology, The Ohio State University, Columbus, Ohio, USA

ABSTRACT The bacterial cell envelope is the first line of defense and point of contact with the environment and other organisms. Envelope biogenesis is therefore crucial for the survival and physiology of bacteria and is often targeted by antimicrobials. Gram-negative bacteria have a multilayered envelope delimited by an inner and outer membrane (IM and OM, respectively). The OM is a barrier against many antimicrobials because of its asymmetric lipid structure, with phospholipids composing the inner leaflet and lipopolysaccharides (LPS) the outer leaflet. Since lipid synthesis occurs at the IM, phospholipids and LPS are transported across the cell envelope and asymmetrically assembled at the OM during growth. How phospholipids are transported to the OM remains unknown. Recently, the *Escherichia coli* protein YhdP has been proposed to participate in this process through an unknown mechanism. YhdP belongs to the AsmA-like clan and contains domains homologous to those found in lipid transporters. Here, we used genetics to investigate the six members of the AsmA-like clan of proteins in *E. coli*. Our data show that YhdP and its paralogs TamB and YdbH are redundant, but not equivalent, in performing an essential function in the cell envelope. Among the AsmA-like paralogs, only the combined loss of YhdP, TamB, and YdbH is lethal, and any of these three proteins is sufficient for growth. We also show that these proteins are required for OM lipid homeostasis and propose that they are the long-sought-after phospholipid transporters that are required for OM biogenesis.

IMPORTANCE Gram-negative bacteria like *Escherichia coli* are characterized by having two membranes. Systems required for the biogenesis of the Gram-negative outer membrane have been identified except for that required for the transport of newly synthesized phospholipids from the inner to the outer membrane. The YhdP protein was previously implicated in this process. Here, we show that YhdP and its homologs TamB and YdbH are redundant in performing an essential function for growth and maintaining lipid homeostasis in the outer membrane. These proteins share a predicted structure with known eukaryotic lipid transporters. Based on our data and previous findings, we propose YhdP, TamB, and YdbH are the missing proteins that transport phospholipids to the outer membrane that have escaped identification because of redundancy.

KEYWORDS AsmA-like proteins, phospholipid transport, outer membrane biogenesis, envelope biogenesis, synthetic lethality

The cell envelope of Gram-negative bacteria contains two essential membranes of distinct composition and function that are separated by an aqueous periplasmic compartment (1, 2). The inner membrane (IM) is a phospholipid bilayer that surrounds the cytoplasm. The outer membrane (OM), which separates the periplasm and the environment, has an inner leaflet composed of phospholipids and an outer leaflet composed of lipopolysaccharides (LPS) (3) (Fig. 1A). The structure and packing of LPS molecules at the cell surface limit the passage of hydrophobic molecules that would

Citation Ruiz N, Davis RM, Kumar S. 2021. YhdP, TamB, and YdbH are redundant but essential for growth and lipid homeostasis of the Gram-negative outer membrane. mBio 12: e02714-21. https://doi.org/10.1128/mBio.02714-21.

Editor Susan Gottesman, National Cancer Institute

Address correspondence to Natividad Ruiz, ruiz.82@osu.edu.

Received 16 September 2021
Accepted 5 October 2021
Published 16 November 2021

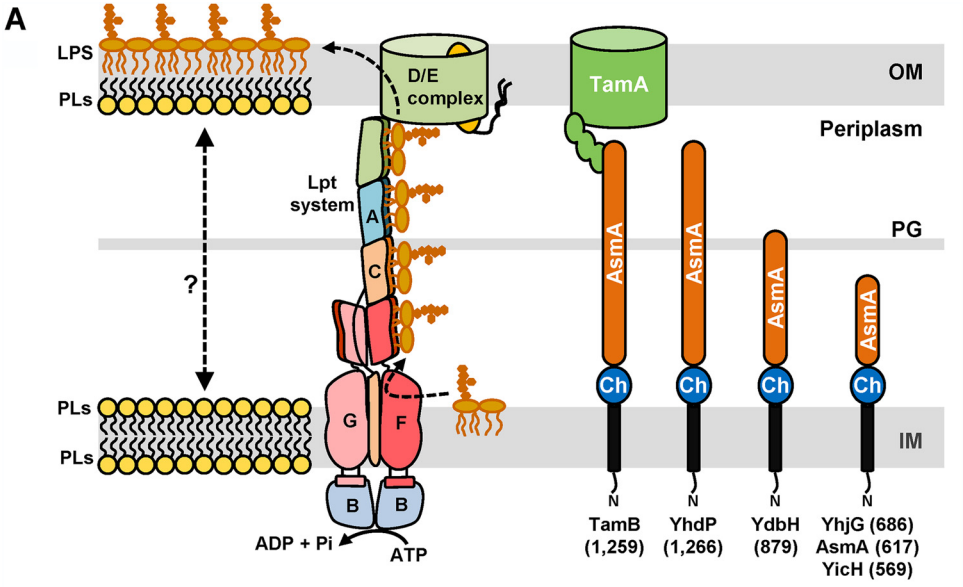

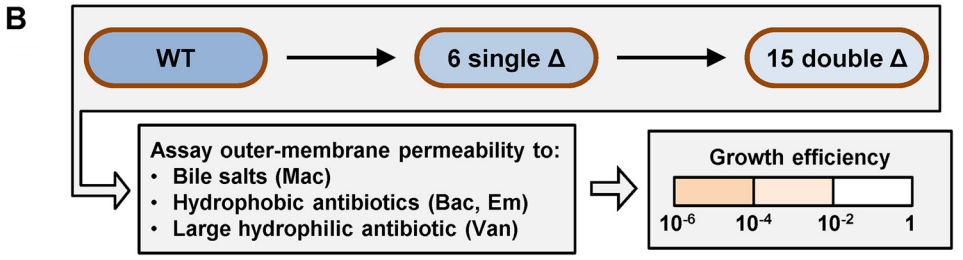

C

Genotype	Efficiency of plating compared to WT in LB				
	LB	Mac	Bac100	Em25	Van75
WT	1.00	1.00	1.00	0.10	1.00
Δ*asmA*	1.00	1.00	1.00	$\leq 10^{-6}$	10^{-3}
Δ*tamB*	1.00	1.00	1.00	0.70 ± 0.52	0.04 ± 0.05
Δ*yhdP*	1.00	1.00	1.00	0.70 ± 0.52	(3.67 ± 5.51) x10^{-5}
Δ*asmA* Δ*tamB*	1.00	1.00	1.00	$\leq 10^{-6}$	10^{-4}
Δ*asmA* Δ*yhdP*	1.00	1.00	1.00	$\leq 10^{-6}$	(6.67 ± 5.77) x10^{-6}
Δ*yhdP* Δ*tamB*	1.00	$\leq 10^{-6}$	$\leq 10^{-6}$	$\leq 10^{-6}$	$\leq 10^{-6}$

FIG 1 TamB and YhdP are functionally redundant for envelope integrity. (A) Cartoon representation of the *E. coli* cell envelope showing the IM and OM, periplasm, and peptidoglycan (PG) layer. On the left, the localization and transport of the major lipid components of the IM and OM are shown. Newly synthesized LPS is transported unidirectionally (dotted arrow) to the outer leaflet of the OM by the Lpt system (LptA-G proteins, labeled A to G), while phospholipids (PLs) are transported bidirectionally (dotted double arrow) between the IM and OM. On the right, cellular localization and predicted domain organization of the six AsmA-like proteins in *E. coli* are shown. Each AsmA-like protein (labeled at the bottom with number of amino acids shown in parentheses) is predicted to be anchored to the IM by an N-terminal transmembrane helix of ca. 22 aa. In the periplasm, they contain a region of ca. 120 aa (Ch) that is homologous to the chorein-N domain found in eukaryotic proteins involved in intermembrane (interorganelle) lipid transporters and a large region varying in length (ca. 425 to 1,125 aa) that is predicted to contain several AsmA domains. TamB has been shown to physically interact with the OM β-barrel protein TamA. (B) Strategy to construct and characterize the 6 mutants lacking one AsmA-like factor (single Δ) and the 15 mutants lacking two of these factors (double Δ). The quality of the barrier function of the OM was assessed by growing all strains in the presence of various antibiotics and bile salts and comparing their growth to that of the wild-type (WT) MG1655 strain in the absence of these compounds (see Materials and Methods for details). (C) Only the Δ*asmA*, Δ*yhdP*, and Δ*tamB* single mutants showed increased OM permeability (see Table S1A). All combinations of two alleles behaved in additive fashion except in the Δ*yhdP* Δ*tamB* double mutant, which exhibited synthetic defective phenotypes (see also Table S1A). Mac refers to MacConkey (bile salts), Bac100, 100 μg/ml bacitracin; Em25, 25 μg/ml erythromycin; Van75, 75 μg/ml vancomycin. Data represent the average and standard deviation from three biological replicates. If not shown, standard deviation equals zero.

otherwise diffuse across phospholipids bilayers. Therefore, the innate resistance of Gram-negative bacteria to hydrophobic antibiotics and detergents depends on the asymmetric assembly of lipids at the OM (4, 5).

During growth, Gram-negative bacteria must expand the IM and OM in coordinated fashion. Since OM lipids are made at the IM (6, 7), growth requires the transport of newly synthesized phospholipids and LPS across the cell envelope (Fig. 1A). Decades ago, Osborn and colleagues demonstrated that, in *Salmonella*, LPS is transported from the IM to the OM, while phospholipids flow bidirectionally between these bilayers (8, 9). Since then, we have learned that LPS is transported across the cell envelope by the Lpt system, a multiprotein complex bridging the IM and OM (1, 10) (Fig. 1A). Lpt functions unidirectionally, as it is powered by an ATP-dependent transporter that moves LPS molecules from the outer leaflet of the IM to the periplasmic Lpt components (11); in addition, LPS translocation across the OM by the LptDE translocon requires activation through a periplasmic domain (12). In contrast, the mechanism for the bidirectional transport of phospholipids remains the most poorly understood essential biogenesis process in the Gram-negative cell envelope. Two types of transport could account for the bidirectional flow of phospholipids between the IM and OM. First, transport could be mediated by protein-based systems spanning the cell envelope (13). Recently, LetB and PqiB have been shown to assemble into tunnel-like structures that have been proposed to bridge the IM and OM and transport phospholipids (14–16). However, their function in cells remains unknown (1, 17). Alternatively, transport could involve hemifusion structures formed by fusion of the outer leaflet of the IM and the inner leaflet of the OM into a contiguous bilayer crossing the periplasm (13). Proteins could still be involved in the latter model by mediating the formation of hemifusion sites and/or cargo selectivity.

Recently, single-cell imaging has shown that IM-to-OM anterograde phospholipid transport occurs by diffusive flow in an *Escherichia coli mlaA** mutant, in which phospholipids are mislocalized from the inner to the outer leaflet of the OM (18, 19). In the Mla system, wild-type MlaA is proposed to remove phospholipids that are somehow mislocalized to the cell surface and transfer them to the periplasmic protein MlaC, which transports them to the MlaBDEF complex to be inserted in the IM in an ATP-dependent manner (20–22). In contrast, MlaA* appears to work in reverse, aberrantly delivering phospholipids to the outer leaflet of the OM (19). In addition, when phospholipids are mislocalized to the cell surface, they can activate the OM phospholipase PldA, which attempts to restore OM lipid asymmetry in two ways: by breaking down the mislocalized phospholipids and by increasing LPS synthesis, likely at the expense of decreasing phospholipid synthesis, through a regulatory cascade that is triggered when the fatty acids released by PldA are recycled into the cytoplasm (23). This strategy contributes to OM lipid homeostasis in wild-type cells. However, when combined with the constitutive mistranslocation of phospholipids to the outer leaflet of the OM in *mlaA** cells, it destabilizes the OM and leads to loss of OM material through blebbing, which further drives the IM-to-OM flow of phospholipids (19). The *mlaA** cells tolerate this increased IM-to-OM flow during exponential growth because lipid synthesis is high; however, when lipid synthesis decreases in stationary phase owing to nutrient limitation, the sustained high demand of IM-to-OM phospholipid transport causes the IM to shrink more and eventually rupture, causing lysis of *mlaA** cells (19). Importantly, a genetic approach enriching for mutations that slow down this anterograde phospholipid transport (i.e., lysis) in *mlaA** cells identified loss-of-function mutations in *yhdP* (18). The rate of lysis of *mlaA* yhdP* cells was shown to be slower than that in the *mlaA** parent because of slower IM shrinking, implicating YhdP in IM-to-OM anterograde phospholipid transport.

The function of YhdP is poorly understood. It was first identified as being required for SDS resistance in carbon-limited *E. coli* (24). In addition, the loss of YhdP causes mild OM permeability defects that can be suppressed by eliminating the synthesis of the cyclic form of enterobacterial common antigen (ECA_{CYC}), a periplasmic glycan of

unknown function (25). However, the effect of YhdP on anterograde phospholipid transport in *mlaA** cells is independent of ECA_{CYC} (18). How YhdP modulates the effect of ECA_{CYC} on OM permeability and phospholipid transport in *mlaA** strains remains unknown, as is whether YhdP affects phospholipid transport in wild-type cells.

It is logical to assume that anterograde phospholipid transport to the OM is essential for growth, since phospholipids are the lipid constituent of the inner leaflet of the OM and the OM is essential for survival. However, YhdP is not essential (24). In addition, the loss of YhdP slows down but does not abolish anterograde phospholipid transport in *mlaA** cells (18). One interpretation of these facts is that YhdP only plays an accessory role in anterograde phospholipid transport. However, its predicted architecture suggests that YhdP directly transports phospholipids. YhdP is a 1,266-residue protein that belongs to the AsmA-like CL0401 protein clan (26). AsmA-like proteins contain a predicted IM-anchoring N-terminal α-helix and a large periplasmic domain that includes a chorein-N domain and the AsmA-like domain (Fig. 1A) (27, 28). Chorein-N domains are present in eukaryotic intermembrane lipid transporters, while AsmA-like domains are composed of various numbers of β-taco domains whose structure resembles that of the domains forming the periplasmic Lpt bridge, which shields the fatty acyl chains of LPS molecules as they travel through the periplasm en route to the OM (Fig. 1A) (29, 30). If YhdP indeed transported phospholipids, it would have to be functionally redundant with other transporters, since it is not essential for viability. Interestingly, *E. coli* encodes YhdP and five additional AsmA-like proteins (TamB [formerly YtfN], YdbH, AsmA, YicH, and YhjG [Fig. 1; see also Fig. S1 in the supplemental material]), and functional redundancy has been suggested as an explanation for why factors involved in IM-to-OM phospholipid transport have remained elusive (1, 31). These connections motivated the present study investigating the possible functional redundancy among AsmA-like proteins in *E. coli*. Using a genetic approach, we found that TamB, YhdP, and YdbH are redundant in performing a function that is essential in envelope biogenesis. We show that the combined loss of TamB, YhdP, and YdbH is lethal, and that mutants lacking five AsmA-like factors grow if they retain either TamB, YhdP, or YdbH. Based on our data and the fact that these proteins are predicted to have domains and overall structures similar to those present in lipid transporters, we propose that TamB, YhdP, and YdbH are the long-sought-after transporters of phospholipids between the IM and OM.

RESULTS

TamB and YhdP are functionally redundant in maintaining the barrier function of the OM. The six paralogs of AsmA-like proteins in *E. coli* contain a chorein-N domain that is present in some intermembrane eukaryotic transporters (see Fig. S1 in the supplemental material). In addition, the recently released AlphaFold Protein Structure Database predicts that they share an overall structure with Atg2, a protein that belongs to a new family of lipid transporters at membrane-contact sites between eukaryotic organelles (Fig. S1) (32–35). Based on these relationships and the fact that YhdP has been shown to affect phospholipid transport from the IM to the OM (18), we investigated a possible role for the AsmA-like protein family in OM biogenesis in *E. coli*. We generated mutants lacking one or more of the six paralogs and tested for defects in growth and OM permeability, as defects in OM structure affects these phenotypes (2, 4). We first characterized the six single mutants. None of them exhibited growth defects in lysogeny broth (LB) at 37°C. To probe OM permeability, we monitored their resistance to bile salts and various antibiotics whose entry is limited by the OM (36). We did not detect OM permeability defects in the Δ*ydbH*, Δ*yhjG*, and Δ*yicH* single mutants, but, as previously reported in various Gram-negative bacteria, the Δ*asmA*, Δ*tamB*, and Δ*yhdP* mutants showed a slight increase in OM permeability (Fig. 1B and C, Table S1A) (24, 25, 37–39).

Next, we constructed mutants carrying multiple deletion alleles to determine if AsmA-like proteins are functionally redundant or function in different or the same pathways. We expected that loss of redundant factors would result in a phenotype

greater than the one expected from adding the phenotype of the single mutants. In contrast, if the effect of combining deletions was additive, it would indicate that the respective factors function in independent pathways. A lack of phenotypic synergy or additivity would be expected if factors functioned in the same pathway. Lastly, a mutant allele might suppress phenotypes conferred by other alleles, revealing that the factors are somehow functionally related. We therefore constructed the 15 double mutants lacking AsmA-like proteins and analyzed the barrier function of their OM (Fig. 1B). We observed that adding either Δ*ydbH*, Δ*yhjG*, or Δ*yicH* to any single mutant did not alter their respective OM permeability phenotypes (Table S1A). Since, on their own, these three alleles do not confer any phenotypes, these analyses did not further clarify the role of YdbH, YhjG, and YicH. In contrast, the three double mutants resulting from combining Δ*asmA*, Δ*tamB*, and Δ*yhdP* revealed key information. The Δ*asmA* allele behaved in an additive fashion with Δ*tamB* and Δ*yhdP* (Fig. 1C, Table S1A), indicating that AsmA performs a function that is different from those of TamB and YhdP. Previously, AsmA had been implicated in the folding of defective integral β-barrel OM proteins (OMPs) (37, 40, 41). Moreover, we uncovered negative synergistic effects between Δ*tamB* and Δ*yhdP*. Unlike the mildly defective single mutants, the Δ*yhdP* Δ*tamB* mutant showed severe OM permeability defects to bile salts and various antibiotics (Fig. 1C). Thus, our characterization suggests that while AsmA works independently, YhdP and TamB function in redundant fashion to maintain the barrier quality of the OM.

TamA is required for TamB's function. TamB forms a complex with the OM β-barrel protein TamA in *E. coli* (Fig. 1A) (42). TamA is a homolog of BamA, the β-barrel component of the BAM complex that assembles β-barrel proteins in the OM (43, 44). In some organisms that lack TamA, TamB has been shown to interact with BamA instead (31, 38). The TAM complex has been proposed to function in the assembly of a subset of OM β-barrel proteins, including autotransporters and fimbrial ushers (29, 42, 45, 46). However, in some organisms, autotransporter biogenesis is not affected by the loss of TamB (47–49), and while biogenesis of autotransporters and ushers requires BAM, they are partially affected in *tamAB* mutants (46, 50). In addition, some bacteria lack autotransporters and fimbrial ushers but possess TamB (and BamA but not TamA) (31, 51). Therefore, the function of TamB remains unclear.

To determine if TamA is required for TamB's function, we analyzed the effects of the Δ*tamA* allele and found that it causes the same phenotypes as Δ*tamB* by itself and in combination with Δ*yhdP* (Table S1B). Furthermore, plasmid-encoded TamB complements Δ*tamB* Δ*yhdP* but not Δ*tamA* Δ*yhdP* with respect to OM permeability defects (Fig. S2A). We therefore conclude that the OM protein TamA is required for TamB's function in maintaining OM permeability.

The combined loss of TamB and YhdP causes pleiotropic defects in the cell envelope. In addition to having OM permeability defects, we observed that cells lacking YhdP and TamB display other phenotypes indicative of severe defects in cell envelope biogenesis. While its parental single mutants grow similarly to the wild type at 37°C in LB, the Δ*yhdP* Δ*tamB* mutant exhibits increased lysis that becomes more evident upon entry into stationary phase (Fig. 2A). Indeed, analysis of concentrated cell-free filtrates from supernatants of overnight cultures showed higher protein content in samples from the Δ*tamB* Δ*yhdP* mutant than the wild-type strain (Fig. 2B). In contrast, samples from the Δ*yhdP* but not the Δ*tamB* single mutant only showed a slight increase in protein content. Furthermore, phase-contrast microscopy of exponentially growing cells showed that the increase in lysis in the Δ*tamB* Δ*yhdP* mutant is not limited to stationary-phase cultures. We could not detect lysis in wild-type and single-mutant cultures, but ghost (i.e., lysed) cells and membrane blebs were readily observed in Δ*tamB* Δ*yhdP* cultures (Fig. 2C and D). Phase-contrast microscopy also revealed that while the overall morphology (length and width) of wild-type and single-mutant cells is similar, Δ*yhdP* Δ*tamB* cells are more irregularly shaped, tending to be shorter and wider than the wild type and single-mutant parents (Fig. 2C to E).

We also observed that, on LB agar, the Δ*yhdP* Δ*tamB* mutant forms mucoid colonies, unlike the parent and wild-type strains (Fig. S3A). Mucoidy results when production of

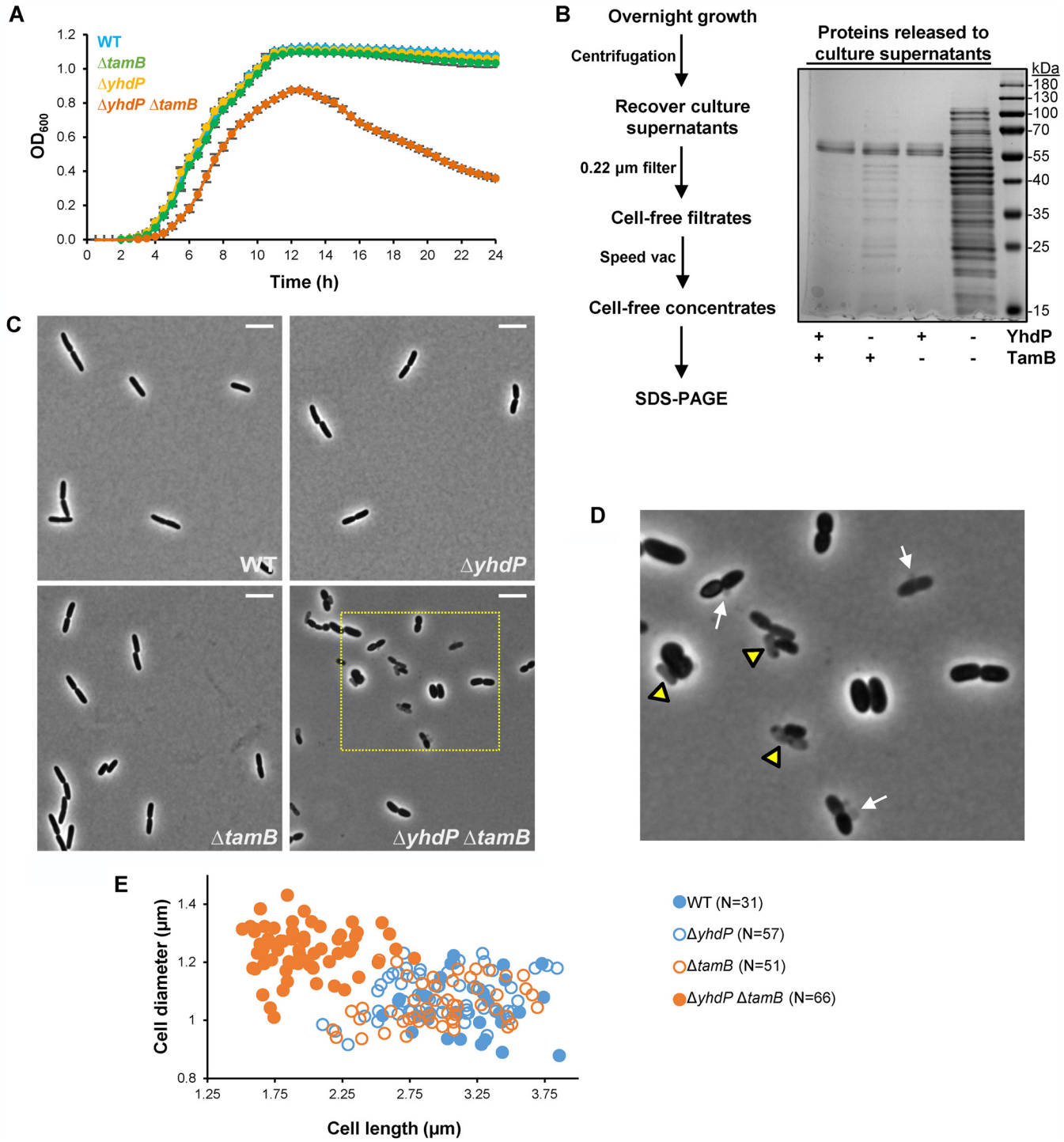

FIG 2 Combined loss of TamB and YhdP synergistically causes lysis and alterations to cellular morphology. (A) Cultures of the Δ*yhdP* Δ*tamB* mutant showed increased lysis, as demonstrated by a drop in optical density (OD_{600}) when growing in LB at 37°C. Data represent the averages and standard deviations from three biological replicates. (B) On the left, scheme showing the experimental strategy to obtain cell-free culture supernatants from overnight cultures grown in LB at 37°C. On the right, SDS-polyacrylamide gel in which proteins were stained with Blue-BANDit after electrophoresis. Gel shown is representative of at least three independent experiments. (C) Phase-contrast microscopy of cells growing in LB at 37°C revealed that loss of either YhdP or TamB alone does not alter cell morphology, but loss of both factors leads to morphological defects. White scale bar (top right) represents 5 μm. Yellow rectangle marks area enlarged in panel D. (D) Δ*yhdP* Δ*tamB* cells exhibit pleiotropic morphological defects: decreased length and increased width, membrane vesiculation or blebbing (white arrows), and increased incidence of lysis (yellow triangles). Images are representative of at least three independent experiments. (E) Cells lacking both YhdP and TamB grow shorter and wider than the wild type and their respective single-mutant parents. The number of cells undergoing constriction after septation (with shape of the number 8) was observed with phase-contrast microscopy, and images were processed with ObjectJ (85) to measure cell length and width of each daughter cell undergoing constriction during exponential growth in LB at 37°C.

colanic acid surface capsule is upregulated by the Rcs envelope stress response via the RcsB response regulator in reaction to various signals, including cell surface stress (52). Capsule production involves the synthesis of intermediates that are linked to undecaprenyl-phosphate, an isoprenoid lipid carrier that is also required for the synthesis of the peptidoglycan cell wall (53). Since the cell wall determines cell shape and protects cells from osmotic lysis, we considered the possibility that lysis and altered cell shape in Δ*yhdP* Δ*tamB* cells could result from titration of undecaprenyl-phosphate from peptidoglycan synthesis by the upregulation of capsule production, as it has been reported when there is an imbalance in the production of polysaccharides whose synthesis rely on undecaprenyl-phosphate (54, 55). To test this possibility, we deleted *rcsB* in the Δ*yhdP* Δ*tamB* mutant. As expected, Δ*rcsB* eliminated mucoidy in the Δ*yhdP* Δ*tamB* mutant; however, the resulting triple mutant still shows increased lysis, severe OM permeability defects, and altered shape (Fig. S3). In fact, Δ*rcsB* worsens the growth of Δ*yhdP* Δ*tamB* cells. This detrimental effect appears to be solely caused by the effect that RcsB has on capsule production, since only deleting a gene responsible for capsule synthesis (*wcaJ*) conferred the same phenotype as Δ*rcsB* (Fig. S3). These results suggest that the Rcs system senses surface stress in Δ*yhdP* Δ*tamB* cells; in agreement, we found that their mucoidy requires the OM lipoprotein sensor RcsF since introduction of Δ*rcsF* abolishes their mucoid phenotype (52). Together, our results indicate that the loss of TamB and YhdP severely compromises the integrity of the cell envelope and that activation of the Rcs envelope-stress response confers some protection by inducing synthesis of a surface polysaccharide capsule.

Lysis of the Δ*tamB* Δ*yhdP* mutant results from defects in OM lipid homeostasis. We have described that cells lacking TamB and YhdP exhibit phenotypes characteristic of OM biogenesis defects: increased permeability to bile salts and antibiotics, production of membrane blebs, and activation of the Rcs response. Not surprisingly, we found that the σ^E stress response is also activated in Δ*yhdP* Δ*tamB* cells (Fig. S4A). The σ^E system regulates synthesis of OM components and OM biogenesis factors in response to stresses, such as the misfolding of OMPs and off-pathway intermediates in LPS transport (56, 57). The OM contains two major types of proteins, OMPs, which fold into β-barrel structures, and lipoproteins, which are anchored to the OM via an N-terminal anchor (58, 59). OMP assembly is catalyzed by the β-barrel assembly machine (BAM), which is composed of the β-barrel protein BamA and the BamB-E lipoproteins (43, 60). Given that both BamA and BamD are essential for BAM function, OMP assembly itself also requires proper biogenesis of OMPs and OM lipoproteins. We therefore analyzed levels and folding of the major OMPs OmpA and OmpC to monitor BAM function and thereby the biogenesis of OMPs and OM lipoproteins. We could not detect misfolding of OmpA and OmpC in cells lacking YhdP and/or TamB (Fig. S4B), suggesting that these proteins do not function in either OMP or lipoprotein biogenesis. We did observe that the Δ*yhdP* Δ*tamB* mutant, unlike its mutant parents, produces higher levels of LPS than the wild type, which might be the cause for the activation of the σ^E stress response if some of the molecules go off pathway (Fig. S4C).

Elevated LPS levels and increased lysis during stationary phase resemble phenotypes previously reported for the *mlaA** mutant (19). As stated earlier, the dominant-negative MlaA* variant causes the mislocalization of phospholipids to the cell surface, which activates PldA, leading to an increase in LPS synthesis and a decrease in phospholipid synthesis (Fig. 3A) (23). The resulting PldA-dependent imbalance in OM lipid synthesis leads to loss of OM material through vesiculation and eventually results in lysis in stationary phase because cells cannot synthesize enough lipids to overcome the loss of OM material (19, 23). Here, we sought to investigate if the stationary-phase-induced lysis in Δ*yhdP* Δ*tamB* mutants was related to defects in the OM. Loss of OM material in *mlaA** cells can be partially suppressed by the addition of Mg^{2+} (19). Similarly, adding 1 mM $MgCl_2$ to the growth medium partially reduces lysis in Δ*yhdP* Δ*tamB* cultures (Fig. S4D), suggesting that lysis in the Δ*yhdP* Δ*tamB* mutant results from the loss of OM material. If so, we expected that Δ*yhdP* Δ*tamB* cells would be hypersensitive to EDTA, since this chelator removes LPS from the cell surface and

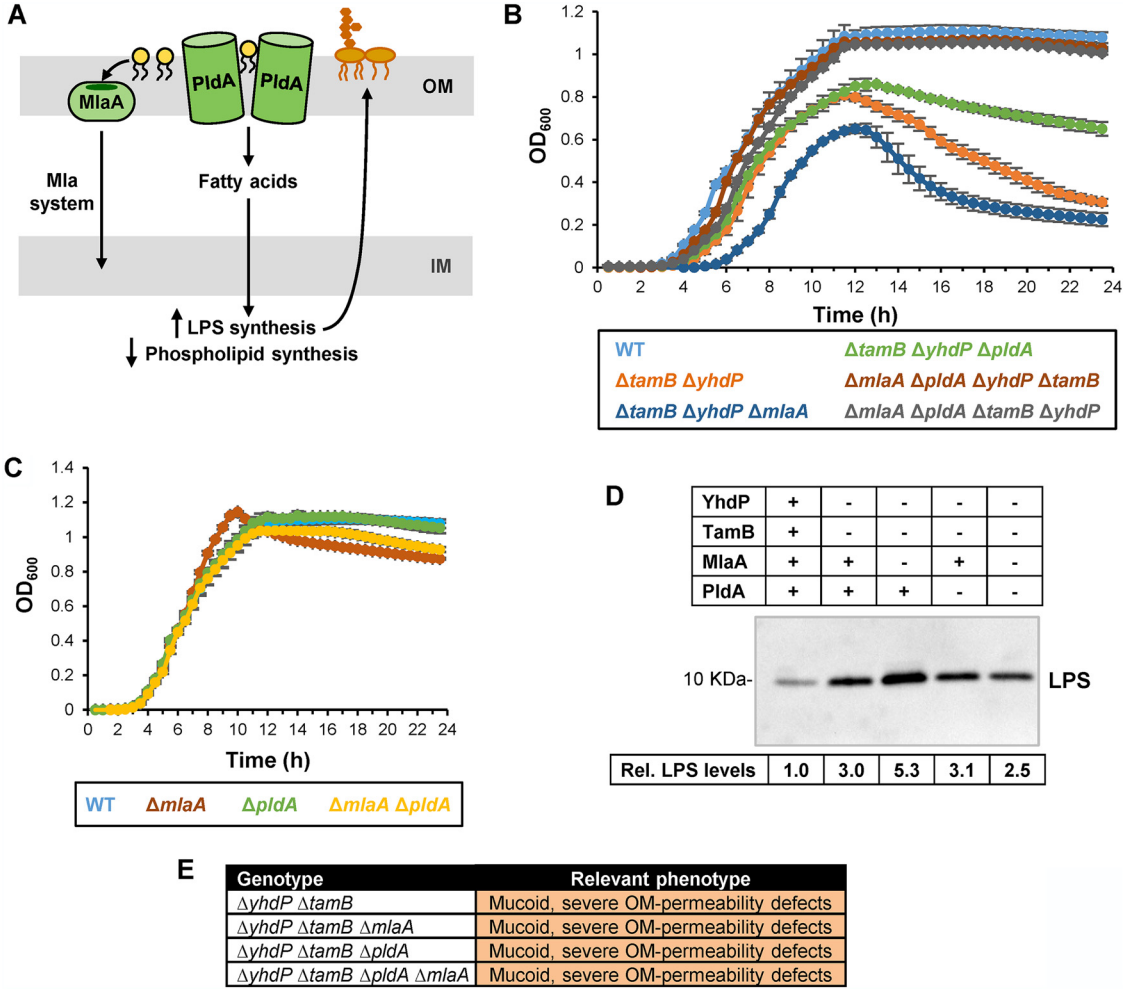

FIG 3 Lysis of the Δ*tamB* Δ*yhdP* mutant results from OM rupture and is suppressed by preventing the removal of phospholipids from the cell surface. (A) Cartoon depicting the function of MlaA and PldA. In wild-type cells, phospholipids mislocalized to the outer leaflet of the OM enter the Mla pathway through MlaA to be transported to the IM. Alternatively, mislocalized phospholipids can be hydrolyzed by a dimer of the PldA phospholipase. The released fatty acyl chains are recycled into the cytoplasm, where they induce higher production of LPS. (B) Growth curves of cultures growing in LB at 37°C. The lysis phenotype of the Δ*yhdP* Δ*tamB* double mutant is enhanced by Δ*mlaA* and partially suppressed by Δ*pldA*. Loss of both PldA and MlaA suppresses the lysis phenotype in the Δ*tamB* Δ*yhdP* mutant. Data represent averages and standard deviations from three biological replicates. (C) Growth curve of wild-type strain MG1655 (WT) and derivatives carrying Δ*mlaA* and/or Δ*pldA* alleles in LB at 37°C. Data represent the averages and standard deviations from three biological replicates. (D) Relative levels of LPS in the wild type and mutants lacking *tamB*, *yhdP*, *mlaA*, and/or *pldA* were measured using immunoblotting from whole-cell samples. Intensity of the signal in the LPS band was measured, and values shown below the immunoblot represent relative values across samples that were calculated by setting levels in the wild-type strain MG1655 to 1.0. (E) Table summarizing mucoidy and OM permeability defects in various strains. For detailed sensitivity data, refer to Table S1C. Data shown in panels D and E are representative of at least three independent experiments.

causes phospholipids to translocate to the outer leaflet of the OM (61). Indeed, the Δ*yhdP* Δ*tamB* mutant is hypersensitive to EDTA (MIC of 0.195 mM compared to 25 mM in the wild-type and single-mutant parents). We also found that adding subinhibitory amounts of EDTA (0.5 mM) to cultures of wild-type and Δ*yhdP* and Δ*tamB* single-mutant strains triggers lysis in stationary phase (Fig. S4D), which is more pronounced in the single mutants than in the wild type. We next explored if MlaA and PldA play a role in the lysis phenotype of Δ*yhdP* Δ*tamB* cells. While deleting *mlaA* increased lysis, deleting *pldA* decreased the rate and extent of lysis induced during stationary phase in Δ*yhdP* Δ*tamB* cells (Fig. 3B and C).

It seemed paradoxical that removing MlaA would have the opposite effect of removing PldA, given that the individual loss of each factor increases the amount of phospholipids at the cell surface. We reasoned that the increase in lysis of Δ*yhdP*

Δ*tamB* cells caused by the loss of MlaA might be dependent on PldA. Specifically, Δ*mlaA* should increase the amount of PldA's substrate (i.e., mislocalized phospholipids), which would upregulate LPS levels while decreasing phospholipid synthesis (23). Indeed, Δ*mlaA* further increases the already elevated LPS levels in a Δ*yhdP* Δ*tamB* mutant (Fig. 3D). We therefore built a Δ*mlaA* Δ*pldA* Δ*yhdP* Δ*tamB* mutant. Strikingly, the combined loss of Δ*mlaA* and Δ*pldA* fully suppresses lysis of Δ*yhdP* Δ*tamB* cells, yielding a wild-type growth pattern (Fig. 3B). As expected, the Δ*mlaA* Δ*pldA* Δ*yhdP* Δ*tamB* mutant also has lower LPS levels than the Δ*yhdP* Δ*tamB* Δ*mlaA* mutant. Nevertheless, the quadruple mutant remains sensitive to bile salts and antibiotics (Fig. 3E, Table S1C).

Together, our results suggest that Δ*yhdP* Δ*tamB* cells have OM structural defects that somehow lead to increased levels of phospholipids in their cell surface, which results in increased sensitivity to bile salts and antibiotics and activation of the Mla and PldA pathways. In Δ*yhdP* Δ*tamB* cells, both MlaA and PldA contribute to lysis by removing these mislocalized phospholipids. PldA's action is particularly detrimental to Δ*yhdP* Δ*tamB* cells because it induces LPS synthesis, causing a further imbalance in OM lipid composition (23). In agreement, adding fatty acids (oleic acid) to the medium exacerbates the lysis phenotype in Δ*yhdP* Δ*tamB* cultures, although a detergent-like effect could also contribute to or cause lysis in these mutant cells (Fig. S4D). If only MlaA is removed, Δ*yhdP* Δ*tamB* cells lyse even more because of PldA's upregulation of LPS levels; however, when both PldA and MlaA are removed, lysis is abolished and cells can grow like the wild type. Thus, these results suggest that TamB and YhdP are required for OM lipid homeostasis.

The AsmA-like protein family is essential for viability in *E. coli*. The main lipid constituents of the OM are LPS and phospholipids. Notably, the Gram-negative *Borrelia* does not produce LPS, yet it encodes *tamB*, which appears to be essential (38). In addition, one of us (N. Ruiz) previously took advantage of the reduced size of two Gram-negative endosymbionts carrying <600 genes to search for envelope biogenesis factors and found *tamB* present in both despite one of these bacteria not having LPS biogenesis genes (51). Here, we expanded this search to five additional gammaproteobacterial endosymbionts and to YhdP. We still found no correlation between the presence of TamB and YhdP and that of LPS biogenesis proteins (Table S2), ruling out a direct role for TamB and YhdP in LPS biogenesis. The fact that these endosymbionts encode either *tamB* or *yhdP* even after having undergone massive gene loss strongly suggests that these proteins perform a crucial function in the physiology of these bacteria. Given that YhdP has been implicated in IM-to-OM transport of phospholipids (18), and its predicted protein architecture supports this proposed role (Fig. S1) (27, 30), the simplest explanation of the evidence presented so far here and by others is that YhdP and TamB mediate phospholipid transport between the IM and OM. However, anterograde phospholipid transport is expected to be essential for building the OM, but even the combined loss of YhdP and TamB is not lethal. We therefore explored if the functional redundancy between TamB and YhdP extends to additional AsmA-like paralogs.

We constructed mutants lacking more than two AsmA-like proteins. Although our data (Fig. 1) suggest that AsmA functions independently of YhdP and TamB, we still included AsmA in our studies. We first combined Δ*yhjG*, Δ*yicH*, and Δ*ydbH* because they do not confer defects individually or in pairs and then introduced Δ*asmA*, Δ*yhdP*, and Δ*tamB*, which on their own confer OM permeability defects. After constructing several mutants, we assayed their OM permeability and compared them to single and double mutants (Fig. 4A, Table S1A) and found that we could not generate a mutant lacking all six AsmA-like proteins (Fig. 4A), suggesting that the AsmA-like family of proteins are essential for viability in *E. coli*.

TamB, YhdP, and YdbH are redundant proteins essential for viability in *E. coli*. Since our genetic analyses indicated that TamB/YhdP and AsmA function in different pathways, we hypothesized that the synthetic lethality observed when attempting to construct a strain lacking all AsmA-like proteins could result from redundancy between TamB/YhdP and YdbH, YicH, and/or YhjG. We found that while the Δ*tamB* Δ*yhdP* Δ*yicH* and Δ*tamB* Δ*yhdP* Δ*yhjG* triple mutants were viable and phenotypically indistinguishable

A

Genotype	Efficiency of plating			
	LB	Bac100	Em25	Van75
WT	1.00	1.00	0.70 ± 0.52	1.00
Δ*yhdP* Δ*tamB*	1.00	≤10^{-6}	≤10^{-6}	≤10^{-6}
Δ*yhjG* Δ*yicH* Δ*ydbH*	1.00	1.00	0.40 ± 0.52	1.00
Δ*yhjG* Δ*yicH* Δ*ydbH* Δ*asmA*	1.00	1.00	≤10^{-6}	(4.00 ± 5.20) x 10^{-4}
Δ*yhjG* Δ*yicH* Δ*ydbH* Δ*tamB*	1.00	1.00	1.00	0.40 ± 0.52
Δ*yhjG* Δ*yicH* Δ*ydbH* Δ*yhdP*	1.00	1.00	1.00	10^{-5}
Δ*yhjG* Δ*yicH* Δ*ydbH* Δ*asmA* Δ*tamB*	1.00	1.00	≤10^{-6}	(3.33 ± 5.77) x 10^{-6}
Δ*yhjG* Δ*yicH* Δ*ydbH* Δ*asmA* Δ*yhdP*	1.00	1.00	≤10^{-6}	(6.67 ± 5.77) x 10^{-6}
Δ*yhjG* Δ*yicH* Δ*ydbH* Δ*asmA* Δ*yhdP* Δ*tamB*	Not viable			
Δ*ydbH* Δ*yhdP* Δ*tamB*	Not viable			

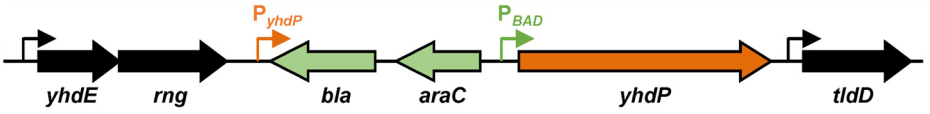

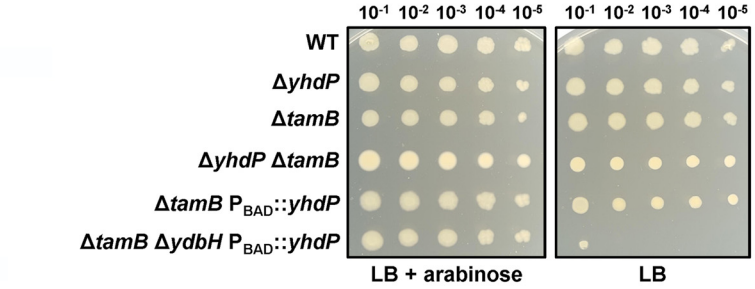

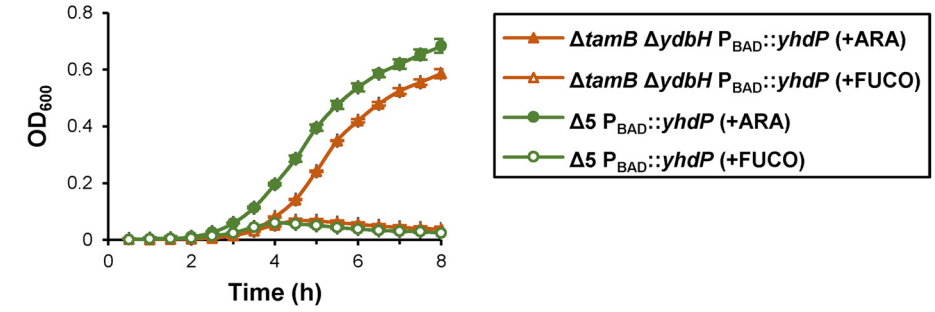

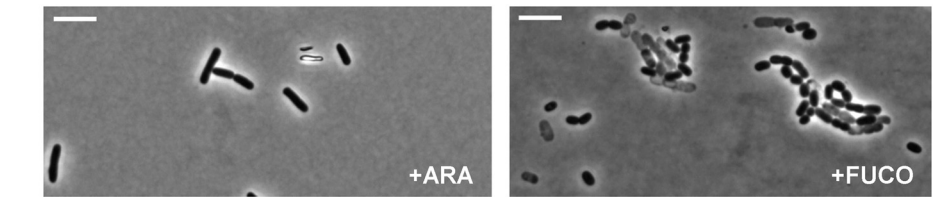

FIG 4 TamB, YhdP, and YdbH are redundant proteins that perform an essential function in *E. coli*. (A) Table showing synthetic genetic interactions resulting from combining deletion alleles of AsmA-like factors. The permeability defects of quintuple mutants only producing either TamB or YhdP resemble those of combining the loss of AsmA and either TamB or YhdP (Fig. 1 and Table S1A). The loss of all AsmA-like factors or the combined loss of TamB, YhdP, and YdbH is lethal. Data represent the average and standard deviation from three biological replicates. If not shown, standard deviation equals zero. (B) Chromosomal *yhdP* locus in YhdP depletion strains. Sequence encoding *bla-araC-*P_{BAD} was inserted upstream of *yhdP* to decouple it from its native promoter (P_{yhdP}). The resulting recombinant locus has been engineered to have *yhdP* transcription under the arabinose-dependent activator AraC. (C) Cultures grown in LB with arabinose overnight at 37°C were diluted 1:10 from left to right and then stamped with a pin replicator onto LB agar containing or lacking arabinose. Growth of the Δ*ydbH* Δ*tamB* P_{BAD}::*yhdP* mutant is arabinose dependent. (D) Depletion of YhdP in a quintuple (Δ5) or a Δ*ydbH* Δ*tamB* double mutant is lethal. Overnight cultures of NR5921 (MG1655 Δ*tamB*::*frt* Δ*ydbH*::*kan yhdP*Ω-1::*bla araC* P_{BAD}) and NR5850 (MG1655 Δ*yhjG*::*frt* Δ*yicH*::*frt* Δ*ydbH*::*frt* Δ*asmA*::*frt* Δ*tamB*::*kan yhdP*Ω-1::*bla araC* P_{BAD}) were grown in LB with arabinose at 37°C. After a 1:5,000 dilution in LB with arabinose (+YhdP) or fucose (YhdP depletion), growth at 37°C was measured by monitoring the OD_{600}. Data represent the average and standard deviation from three biological replicates. (E) Phase-contrast microscopy (100× objective) of strain NR5921 grown in the presence of arabinose or fucose. White scale bar represents 5 μm. Data are representative of at least three independent experiments.

from the Δ*tamB* Δ*yhdP* mutant, we could not build the Δ*tamB* Δ*yhdP* Δ*ydbH* triple mutant (Fig. 4A), suggesting these three alleles are synthetic lethal.

We next constructed a YhdP depletion strain to better test if Δ*tamB*, Δ*yhdP*, and Δ*ydbH* are synthetically lethal. By altering its promoter region, we placed *yhdP* transcription under the control of the arabinose-inducible promoter P_{BAD} (Fig. 4B) (62). We confirmed that expression of *yhdP* is controlled by arabinose in strains carrying P_{BAD}::*yhdP* by showing that a Δ*tamB* P_{BAD}::*yhdP* strain exhibits OM permeability defects similar to those of a Δ*tamB* Δ*yhdP* mutant when grown in the presence of the anti-inducer D-fucose (an L-arabinose analog) but not in the presence of the inducer arabinose (Fig. S5A and B). Next, we constructed a Δ*tamB* Δ*ydbH* P_{BAD}::*yhdP* strain in the presence of arabinose and determined that its growth is arabinose dependent (Fig. 4C and D). Thus, Δ*tamB*, Δ*yhdP*, and Δ*ydbH* are indeed synthetically lethal. We also built a YhdP depletion strain lacking the genes encoding the other five AsmA-like proteins and determined that it behaves similarly to the Δ*tamB* Δ*ydbH* P_{BAD}::*yhdP* strain (Fig. 4D). Further characterization of the Δ*tamB* Δ*ydbH* P_{BAD}::*yhdP* strain showed that growth in the presence of D-fucose does not cause defects in the assembly of the major β-barrel protein OmpA but induces production of DegP, which is controlled by the σ^E stress response (56), and LPS (Fig. S5). Phase-contrast microscopy revealed that, in the presence of arabinose, the Δ*tamB* Δ*ydbH* P_{BAD}::*yhdP* strain cells appear like wild-type rods, but, in the presence of fucose, the depletion strain undergoes lysis and exhibits morphological defects (Fig. 4E).

Given that the combined loss of *mlaA* and *pldA* suppresses lysis in Δ*tamB* Δ*yhdP* cells, we tested if it could also suppress the dependence on arabinose for growth of the Δ*tamB* Δ*ydbH* P_{BAD}::*yhdP* strain. We found that it could not (Fig. S5F). However, we showed that TamA is essential in cells lacking YhdP and YdbH, confirming our earlier conclusion that TamA is required for TamB function (Fig. S2B). Altogether, our data demonstrate that TamB, YhdP, and YdbH are redundant in performing a function that is essential for growth of *E. coli*. Nevertheless, the difference in phenotypes observed in the three Δ*tamB*, Δ*yhdP*, and Δ*ydbH* single mutants, and their corresponding double and triple mutants, also suggest that despite being functionally redundant, these proteins are not equivalent (Table S1A).

Gain-of-function substitutions in YdbH suppress defects in the Δ*tamB* Δ*yhdP* mutant. We next searched for suppressor mutations that could provide information about the function of TamB, YhdP, and YdbH using both reverse and forward genetics. We focused on isolating suppressors of the Δ*tamB* Δ*yhdP* double mutant. For the reverse-genetic approach, we tested whether the loss of the enterobacterial common antigen (ECA) caused by deleting *wecA* could suppress the increase in OM permeability and/or lysis, since, as stated earlier, it suppresses OM permeability defects in a Δ*yhdP* mutant (25). We did not observe changes in OM permeability in either the wild-type or the Δ*tamB* mutant, but, as previously reported, observed that Δ*wecA* suppresses the sensitivity of a Δ*yhdP* mutant to vancomycin (Table S1D) (25). However, Δ*wecA* does not suppress the OM permeability defects in the Δ*tamB* Δ*yhdP* mutant and, in fact, severely compromises its growth (Table S1D and data not shown). Thus, the ability of the loss of ECA to suppress the OM permeability defects caused by Δ*yhdP* requires TamB, and losing ECA has a detrimental effect on the fitness of Δ*tamB* Δ*yhdP* cells.

We next employed an unbiased selection for spontaneous mutants that restore growth of the Δ*tamB* Δ*yhdP* mutant in the presence of bile salts (i.e., MacConkey agar). After mapping suppressor mutations by genetic linkage, we identified four different missense mutations in *ydbH* that change conserved residues in the periplasmic region of YdbH, T303I, G305W, G308C, and G456V (Fig. 5). We found that these missense *ydbH* alleles also decrease sensitivity to hydrophobic antibiotics, but not vancomycin (Fig. 5B). Thus, these suppressor mutations do not fully restore wild-type phenotypes. Given that the loss of YdbH is lethal in the Δ*tamB* Δ*yhdP* mutant, we expected these alleles to be gain-of-function alleles. In agreement with these alleles being gain of function and not loss of function, introducing a plasmid carrying the wild-type *ydbH* locus also restores growth of the Δ*tamB* Δ*yhdP* mutant on MacConkey agar. Thus, altering YdbH function through mutations or increasing levels of wild-type YdbH function suppresses sensitivity

A

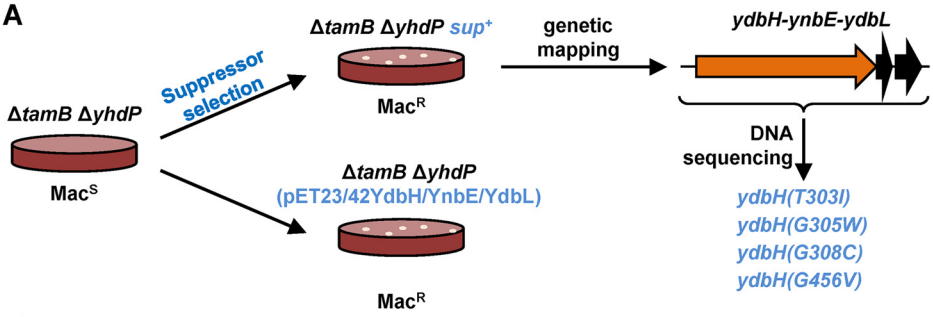

B

Genotype	Efficiency of plating compared to WT in LB				
	LB	Mac	Bac100	Em25	Van75
WT	1.00	0.40 ± 0.52	0.40 ± 0.52	0.70 ± 0.52	0.1
Δ*yhdP* Δ*tamB*	0.07 ± 0.05	≤10^{-6}	≤10^{-6}	(4.0 ± 5.2) x 10^{-4}	≤10^{-6}
Δ*yhdP* Δ*tamB ydbH(T303I)*	0.10	0.04 ± 0.05	0.04 ± 0.05	0.70 ± 0.52	≤10^{-6}
Δ*yhdP* Δ*tamB ydbH(G305W)*	0.70 ± 0.52	0.07 ± 0.05	0.10	0.40 ± 0.52	≤10^{-6}
Δ*yhdP* Δ*tamB ydbH(G308C)*	0.10	0.04 ± 0.05	0.37 ± 0.55	0.10	≤10^{-6}
Δ*yhdP* Δ*tamB ydbH(G456V)*	0.40 ± 0.52	0.04 ± 0.05	0.34 ± 0.57	0.10	≤10^{-6}

C

Residue	Cons. score	Residue variety	Suppressor change
V301	6	L,M,I,A,V	
L302	6	R,V,I,T,Q,M,L	
T303	9	S,T	I
Q304	5	A,N,R,E,T,K,H,G,S,Q,D	
G305	8	S,G,A,N	W
Q306	2	T,L,N,R,E,A,Q,D,I,G,S,V,H,K	
A307	7	H,K,F,Q,G,S,N,R,E,A,T,L	
G308	9	G	C
K309	9	I,K,R	
G310	7	G,S,A	
D451	9	T,N,R,S,Q,D,K,H	
V452	7	M,I,G,L,V,F	
A453	3	A,R,N,E,M,T,K,V,H,G,S,Q,D	
G454	9	G,S	
K455	2	E,R,N,A,T,Y,L,H,V,K,D,I,Q,S	
G456	9	G	V
E457	3	D,Q,S,G,H,V,F,K,Y,M,L,E,N,R,A	
W458	9	I,W	
H459	3	H,V,K,D,I,Q,S,E,R,N,A,L	
D460	6	D,Q,G,H,Y,E,N,R,A	

D

FIG 5 Gain-of-function substitutions in YdbH suppress defects in the Δ*tamB* Δ*yhdP* mutant. (A) Suppressors of the sensitivity of the Δ*tamB* Δ*yhdP* double mutant to bile salts were selected on MacConkey (Mac) agar. Suppressor mutations are missense mutations in *ydbH*. Introduction of a plasmid carrying the *ydbH-ynbE-ydbL* locus into the Δ*tamB* Δ*yhdP* mutant also suppresses its inability to grow on MacConkey agar. (B) Missense mutations in *ydbH* suppress OM permeability defects in the Δ*tamB* Δ*yhdP* double mutant. Data represent the average and standard deviation from three biological replicates. If not shown, standard deviation equals zero. (C) Suppressor mutations in *ydbH* alter residues that are highly conserved among 288 unique YdbH homologs. Table shows Consurf (86) conservation scores (Cons. score) of residues in the regions where suppressing changes are localized in YdbH. Conservation scale ranges from 1 (most variable) to 9 (most conserved). Although these residues are conserved among YdbH orthologs, they are not conserved at the same positions in YhdP and TamB. (D) Model structure (see Fig. S1) of YdbH showing residues altered by suppressor mutations as green spheres. The cluster containing residues 303, 305, and 308 is located in a loop, while the side chain of residue 456 faces the interior of the tubular AsmA-like domain.

to bile salts (Fig. 5A). Further characterization will be needed to understand how these changes suppress defects in Δ*tamB* Δ*yhdP* cells, but they support our conclusion that TamB, YhdP, and YdbH are functionally redundant but not equivalent.

DISCUSSION

The AsmA-like family of proteins has been recognized as conserved and specific to didermic Gram-negative bacteria, but determining its function has been difficult. The fact that many organisms, including *E. coli*, the model bacterium for studying the Gram-negative envelope, encode up to six AsmA-like paralogs (TamB, YhdP, YdbH, AsmA, YicH, and YhjG) has limited progress for our understanding of this protein family

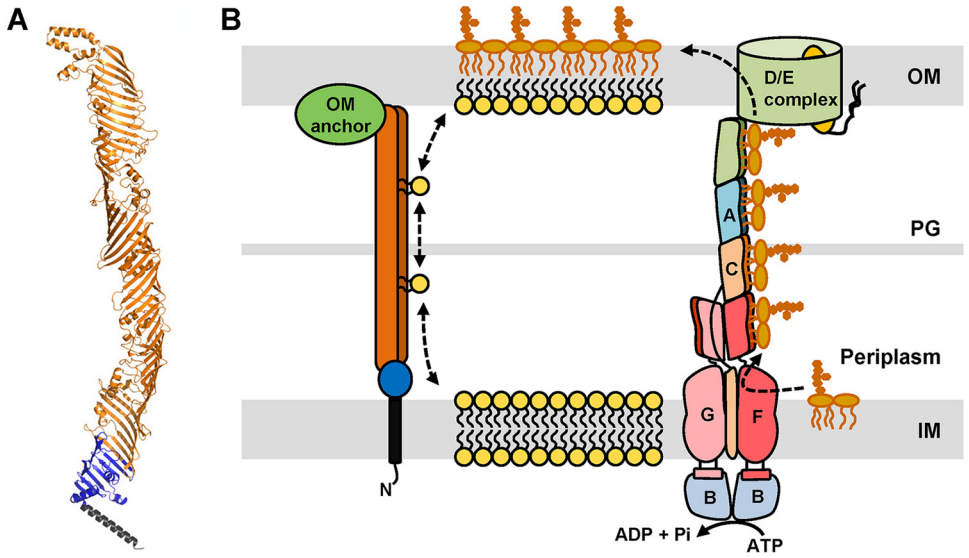

FIG 6 Model of OM lipid assembly. (A) Cartoon representation of the structural prediction for YhdP by AlphaFold (32). Regions of the structural model are colored as in Fig. 1A, with the transmembrane helix in black, the chorein-N domain in blue, and the AsmA domain in orange. (B) Model of OM lipid transport and assembly. The Lpt system (on the right) transports newly synthesized LPS molecules from the IM to the outer leaflet of the OM. We propose that TamB, YhdP, and YdbH transport phospholipids between the IM and OM. In this model, TamB, YhdP, and YdbH physically bridge the IM and OM by anchoring to the IM through their N-terminal α-helix (black segment) and likely to the OM via interactions with partners (green oval). The predicted structure of the large periplasmic region of these proteins would form a structure similar to the Lpt bridge and provide protection to the hydrophobic fatty acid chains of phospholipids as they travel through the periplasm. LPS transport is unidirectional and powered by ATP, while bidirectional phospholipid transport would be driven by diffusion through TamB, YhdP, and YdbH.

(31). Indeed, although previous studies have linked AsmA, TamB, and YhdP to envelope biogenesis in various bacteria, their role remains mostly uncharacterized (18, 24, 25, 28, 37–42, 45, 47–49). To investigate whether redundancy was occluding their function in *E. coli*, we used reverse genetics to generate and characterize mutants lacking one or several AsmA-like proteins. Our work demonstrates that TamB, YhdP, and YdbH are redundant in performing a function that is critical for OM lipid homeostasis and essential for growth.

Previously, YhdP had been implicated in diffusive anterograde phospholipid transport between the IM and OM in *mlaA* E. coli* mutants, which have altered OM lipid structure (18). However, its role in anterograde phospholipid transport in wild-type cells remained unclear, especially because the loss of YhdP results in mild phenotypes but anterograde phospholipid transport is presumed to be essential for building the OM and thereby growth (24, 25). Our work addresses these issues by showing that the combined loss of YhdP, TamB, and YdbH is lethal in an otherwise wild-type strain because these proteins are crucial in maintaining lipid homeostasis at the OM (Fig. 3 and 4). This essential role for growth is also underscored by the fact that at least one of these proteins is conserved in Gram-negative endosymbionts that encode fewer than 600 proteins in their reduced-size genomes (Table S2) (51). Importantly, TamB, YhdP, and YdbH are homologous to the eukaryotic proteins Vps13 and Atg2, which were recently shown to constitute a new family of lipid transporters at membrane-contact sites between organelles (33–35, 63), and the less-characterized TIC236 and Mdm31/32 homologs, which are also needed for proper biogenesis of chloroplasts and mitochondria, respectively (27, 30, 33–35, 63–65). Given this body of evidence and that anterograde IM-to-OM phospholipid transport is the only essential process required for OM biogenesis that is yet to be linked to the essentiality of any protein(s) (1), we propose that TamB, YhdP, and YdbH transport phospholipids between the IM and OM (Fig. 6).

Transport of phospholipids between the IM and OM has been proposed to occur by diffusion mediated either by proteinaceous bridge-like structures or by lipid bilayer

structures fusing the IM and OM (1, 9, 13, 18, 19, 66, 67). In the latter model, TamB, YhdP, and YdbH could be responsible for building or maintaining the proposed membrane bridges or for preventing the flow and mislocalization of proteins or lipid-linked molecules between the IM and OM. However, based on the predicted architecture of their homologs, Vps13 and Atg2, and the structural models recently released by AlphaFold (Fig. S1) (32), we favor a model in which TamB, YhdP, and YdbH are proteinaceous bridges between the IM and OM that directly facilitate the flow of phospholipids (Fig. 6). Vps13 and Atg2 are large intermembrane bridge proteins that are anchored to the membrane of one organelle via an N-terminal α-helix; this anchor is then followed by a chorein-N domain, a large region rich in β-strands, and variable domains that are thought to mediate interactions with different factors at the membrane of another organelle (30, 33, 63, 64, 68). The large region rich in β-strands bridging the two membranes is modeled to fold into a structure that resembles the periplasmic bridge formed by the Lpt proteins that transports the glycolipid LPS from the IM to the OM (11, 69, 70) (Fig. 6). Specifically, they are thought to form an elongated tube-like structure with a lateral opening along the long axis that leads to a hydrophobic groove that interacts with phospholipids by protecting the hydrophobic fatty acid tails of multiple lipids as they travel through aqueous compartments from one membrane to another (33, 68). TamB, YhdP, and YdbH also have an N-terminal α-helix that is followed by a chorein-N domain and a large portion rich in β-strands ($>$700 amino acids [aa]) large enough to cross the periplasm (27). Their structure is predicted to resemble that of Atg2 (Fig. S1). The eukaryotic homologs Vps13 and Atg2 contact two membranes from different organelles and associate with various partners through their C-terminal domains (30, 64). To date, no partners have been identified for YhdP and YdbH, but TamB interacts, depending on the organism, with the OMP TamA or BamA (31, 38, 42). In agreement, our data show that TamA is required for TamB's function (Table S1B and Fig. S2). Based on the TamB-TamA interaction and that of their eukaryotic homologs with their partners, we propose that YhdP and YdbH are also likely to require an OM anchor (Fig. 6). We therefore suggest that TamB, YhdP, and YdbH constitute the membrane-contact sites proposed decades ago to mediate phospholipid transport between the IM and OM (66, 67, 71). In this model, TamB, YhdP, and YdbH would provide a bridge-like structure resembling that of the Lpt bridge that protects phospholipids as they travel across the periplasm (Fig. 6). However, unlike the unidirectional LPS transport mediated by the Lpt system, TamB, YhdP, and YdbH would support the previously reported bidirectional diffusive flow of phospholipids (Fig. 6) (9, 18, 19, 66, 67).

Functional redundancy between TamB, YhdP, and YdbH would also explain why the identification of the mechanism for anterograde phospholipid transport has remained elusive despite the great progress made in the identification and characterization of factors involved in the biogenesis of other envelope components (1, 13). Nevertheless, even though our data show that TamB, YhdP, and YdbH are redundant and any of them is sufficient to support growth of *E. coli*, these proteins are not functionally equivalent. Instead, our phenotypic analysis of the respective single and double mutants has revealed a functional hierarchy in the cell envelope that correlates with protein size (Fig. 1): TamB and YhdP play a more similar and important role than YdbH. The nature of this specialization is unknown, but possible explanations include differences in expression, cargo preference, and/or cellular localization as it occurs among the four human Vps13 paralogs (64). It is also possible that the specialization of these paralogs results from additional different functions that these proteins have evolved to perform. For example, TamB has been shown to affect the transport of a nonconserved subset of β-barrel proteins from the IM to the OM (28, 29, 42, 46). Whether this is an additional function of TamB or a secondary effect of the loss of its primary role in OM lipid biogenesis needs to be determined.

Lastly, we note that growth of the OM lipid bilayer requires the balanced assembly of phospholipids at the inner leaflet and of LPS and other lipid-linked oligosaccharides

at the outer leaflet of the OM (1). How the synthesis, transport, and assembly of these lipid components are coordinated is poorly understood, but studies like ours and those previously done on *mlaA** show that imbalance leads to severe defects in asymmetry and even death when the growth of the two leaflets of the OM is out of balance (18, 19). In *mlaA** mutants, growth of the inner leaflet of the OM is compromised because of the aberrant translocation of phospholipids to the cell surface, which, in turn, causes the activation of PldA and downstream upregulation of LPS synthesis. These two events increase the synthesis of the main lipid component of the outer leaflet (LPS) and decrease the presence and synthesis, respectively, of the main lipid component of the inner leaflet (phospholipids). In our study, we found that a Δ*tamB* Δ*yhdP* mutant undergoes lysis that is suppressed by the loss of MlaA and PldA (Fig. 3). We propose that the compromised flow of phospholipids to the OM in the Δ*tamB* Δ*yhdP* mutant disrupts OM lipid homeostasis, somehow also leading to the activation of PldA and the subsequent upregulation of LPS synthesis. Upregulating the production of the main component of the outer leaflet of the OM (LPS) likely harms the cell through a futile cycle in which the LPS-driven growth of the outer leaflet of the OM would increase the demand for an already compromised transport of phospholipids, further driving the disruption of OM lipid homeostasis. How phospholipids are translocated across the OM in wild-type and Δ*tamB* Δ*yhdP* cells also remains unknown. Recent studies are just beginning to reveal how OM lipid asymmetry and LPS transport may be sensed by PldA and YejM to coordinate the synthesis of phospholipids and LPS through the regulated degradation of the LPS synthesis enzyme LpxC by FtsH/LepB (72–77). Our work calls for investigating how TamB, YhdP, and YdbH may be integrated in these systems, as well as the role that other surface components such as ECA and capsule may play.

MATERIALS AND METHODS

Bacterial strains. Strains were derived from wild-type strain MG1655 (78) and are listed in Table S3A in the supplemental material. Deletion alleles were derived from the Keio collection (79) and introduced into the appropriate strains by generalized P1vir transduction and selection for kanamycin resistance (80). When necessary, kanamycin resistance cassettes were excised by the Flp recombinase as previously described (81). Unless indicated, strains were grown in LB medium at 37°C either in liquid cultures with aeration or on solid medium containing 1.5% agar (80). When necessary, growth media were supplemented with ampicillin (25 or 125 μg/ml), L-arabinose (0.2%, wt/vol), bacitracin (100 μg/ml), chloramphenicol (20 μg/ml), erythromycin (25 μg/ml), vancomycin (25 or 75 μg/ml), kanamycin (25 μg/ml), tetracycline (25 μg/ml), $MgCl_2$ (1 mM), EDTA (0.5 mM), oleic acid (10 mg/ml). MacConkey agar was commercially available from BD (catalog no. BD281810). Except for YhdP depletion strains, to monitor growth of strains, overnight cultures were diluted 1:1,000 in LB with the appropriate additives. Diluted cultures were delivered (200 μl) into a 96-well plate that was incubated at 37°C with continuous double orbital shaking in an Epoch2 BioTek reader. Growth was monitored every 30 min by measuring absorbance at 600 nm (OD_{600}).

YhdP depletion. A YhdP depletion strain was constructed by recombineering as previously described (51). Briefly, primers 5YhdP_Pbad and YhdP_Pbad (Table S3B) were used to amplify the *bla-araC*-P_{BAD} region of pKD46 (82). The PCR product was used for recombineering to insert *bla-araC*-P_{BAD} between the −1 and +1 positions of the *yhdP* gene in the chromosome of the recombineering strain DY378 (83). Recombinants were selected at 30°C on medium containing 25 μg/ml ampicillin and confirmed by PCR analysis. The *yhdP* Ω(−1:: *bla araC*-P_{BAD}) allele was introduced into various strains by using $P1_{vir}$ transduction (80) by selecting ampicillin-resistant transductants. To deplete YhdP, cells grown overnight in LB with arabinose were washed once in LB and diluted 1:5,000 (vol/vol) in 25 ml LB with arabinose (+YhdP) or fucose (YhdP depletion) and grown at 37°C with shaking. Growth was monitored by measuring the OD_{600}. For depletion on solid medium, overnight cultures grown in the presence of arabinose were serially diluted 1:10 in LB and stamped with a 48-pin replicator on the appropriate plates containing or lacking arabinose.

Efficiency of plating assay. Cultures grown overnight at 37°C in LB were serially diluted 1:10 (vol/vol). Dilutions were transferred with a 48-pin replicator to various plates and incubated overnight at 37°C. Efficiency of plating values was calculated by dividing the highest dilution with growth for each strain under each condition by the highest dilution with growth for that the wild-type strain MG1655 on LB agar.

EDTA sensitivity assay. Cultures grown overnight at 37°C in LB were diluted 1:1,000 (vol/vol) in LB and delivered to 96-well plates. EDTA was added and serially diluted to generate a 1:2 range of concentrations. After overnight incubation at 37°C, the MIC was determined as the lowest concentration of EDTA that inhibited growth as determined by OD_{600}.

Microscopy. Cells grown in liquid media as indicated in each experiment were layered on a 1% agarose pad in LB and imaged using phase-contrast with a 100× oil immersion lens objective and a Nikon

Eclipse Ti-E microscope equipped with a Nikon DS-QI1 cooled digital camera. See the supplemental material for details about cell measurements.

Suppressor selection and mapping. MacConkey-resistant suppressors were selected by plating 1 to 2 ml of overnight cultures of NR5161 on MacConkey agar plates. Selection plates were incubated overnight at 37°C. The *ydbH* suppressor alleles were mapped by $P1_{vir}$ cotransduction frequency to tetracycline-resistant mini-Tn markers as described previously (84). Suppressor mutations were identified by amplifying the chromosomal *ydbH* locus via PCR and sequencing the resulting PCR product. A linked *tet2-3* mini-Tn insertion [IGR(*ynaE-uspF*)::*tet*] was used to move *ydbH* suppressor alleles into various strains via $P1_{vir}$ transduction and demonstrate that they are solely responsible for suppression.

SUPPLEMENTAL MATERIAL

Supplemental material is available online only.

TEXT S1, DOCX file, 0.1 MB.

FIG S1, PDF file, 0.8 MB.

FIG S2, PDF file, 0.6 MB.

FIG S3, TIF file, 1.8 MB.

FIG S4, TIF file, 1.8 MB.

FIG S5, TIF file, 2.8 MB.

TABLE S1, XLSX file, 0.02 MB.

TABLE S2, PDF file, 0.1 MB.

TABLE S3, XLSX file, 0.02 MB.

ACKNOWLEDGMENTS

This study was supported by the National Institute of General Medical Sciences award GM100951 and the National Institute of Allergy and Infectious Diseases award AI139271 (to N.R.).

We declare that we have no competing interest.

REFERENCES

1. Lundstedt E, Kahne D, Ruiz N. 2021. Assembly and maintenance of lipids at the bacterial outer membrane. Chem Rev 121:5098–5123. https://doi.org/10.1021/acs.chemrev.0c00587.
2. Silhavy TJ, Kahne D, Walker S. 2010. The bacterial cell envelope. Cold Spring Harb Perspect Biol 2:a000414. https://doi.org/10.1101/cshperspect.a000414.
3. Kamio Y, Nikaido H. 1976. Outer membrane of *Salmonella typhimurium*: accessibility of phospholipid head groups to phospholipase c and cyanogen bromide activated dextran in the external medium. Biochemistry 15:2561–2570. https://doi.org/10.1021/bi00657a012.
4. Nikaido H. 2003. Molecular basis of bacterial outer membrane permeability revisited. Microbiol Mol Biol Rev 67:593–656. https://doi.org/10.1128/MMBR.67.4.593-656.2003.
5. Lehman KM, Grabowicz M. 2019. Countering Gram-negative antibiotic resistance: recent progress in disrupting the outer membrane with novel therapeutics. Antibiotics 8:163. https://doi.org/10.3390/antibiotics8040163.
6. Parsons JB, Rock CO. 2013. Bacterial lipids: metabolism and membrane homeostasis. Prog Lipid Res 52:249–276. https://doi.org/10.1016/j.plipres.2013.02.002.
7. Bertani B, Ruiz N. 2018. Function and biogenesis of lipopolysaccharides. EcoSal Plus 8:10.1128/ecosalplus.ESP-0001-2018. https://doi.org/10.1128/ecosalplus.ESP-0001-2018.
8. Osborn MJ, Gander JE, Parisi E. 1972. Mechanism of assembly of the outer membrane of *Salmonella typhimurium*. Site of synthesis of lipopolysaccharide. J Biol Chem 247:3973–3986. https://doi.org/10.1016/S0021-9258(19)45128-4.
9. Jones NC, Osborn MJ. 1977. Interaction of *Salmonella typhimurium* with phospholipid vesicles. Incorporation of exogenous lipids into intact cells. J Biol Chem 252:7398–7404. https://doi.org/10.1016/S0021-9258(19)66978-4.
10. Sherman DJ, Xie R, Taylor RJ, George AH, Okuda S, Foster PJ, Needleman DJ, Kahne D. 2018. Lipopolysaccharide is transported to the cell surface by a membrane-to-membrane protein bridge. Science 359:798–801. https://doi.org/10.1126/science.aar1886.
11. Owens TW, Taylor RJ, Pahil KS, Bertani BR, Ruiz N, Kruse AC, Kahne D. 2019. Structural basis of unidirectional export of lipopolysaccharide to the cell surface. Nature 567:550–553. https://doi.org/10.1038/s41586-019-1039-0.
12. Fiorentino F, Sauer JB, Qiu X, Corey RA, Cassidy CK, Mynors-Wallis B, Mehmood S, Bolla JR, Stansfeld PJ, Robinson CV. 2021. Dynamics of an LPS translocon induced by substrate and an antimicrobial peptide. Nat Chem Biol 17:187–195. https://doi.org/10.1038/s41589-020-00694-2.
13. Wilson A, Ruiz N. 2021. Transport of lipopolysaccharides and phospholipids to the outer membrane. Curr Opin Microbiol 60:51–57. https://doi.org/10.1016/j.mib.2021.01.006.
14. Ekiert DC, Bhabha G, Isom GL, Greenan G, Ovchinnikov S, Henderson IR, Cox JS, Vale RD. 2017. Architectures of lipid transport systems for the bacterial outer membrane. Cell 169:273–285. https://doi.org/10.1016/j.cell.2017.03.019.
15. Isom GL, Coudray N, MacRae MR, McManus CT, Ekiert DC, Bhabha G. 2020. LetB structure reveals a tunnel for lipid transport across the bacterial envelope. Cell 181:653–664. https://doi.org/10.1016/j.cell.2020.03.030.
16. Liu C, Ma J, Wang J, Wang H, Zhang L. 2020. Cryo-EM structure of a bacterial lipid transporter YebT. J Mol Biol 432:1008–1019. https://doi.org/10.1016/j.jmb.2019.12.008.
17. Powers MJ, Trent MS. 2020. Aboard the LetB express. Nat Struct Mol Biol 27:403–405. https://doi.org/10.1038/s41594-020-0431-7.
18. Grimm J, Shi H, Wang W, Mitchell AM, Wingreen NS, Huang KC, Silhavy TJ. 2020. The inner membrane protein YhdP modulates the rate of anterograde phospholipid flow in *Escherichia coli*. Proc Natl Acad Sci U S A 117:26907–26914. https://doi.org/10.1073/pnas.2015556117.
19. Sutterlin HA, Shi H, May KL, Miguel A, Khare S, Huang KC, Silhavy TJ. 2016. Disruption of lipid homeostasis in the Gram-negative cell envelope activates a novel cell death pathway. Proc Natl Acad Sci U S A 113:E1565–E1574. https://doi.org/10.1073/pnas.1601375113.
20. Shrivastava R, Chng SS. 2019. Lipid trafficking across the Gram-negative cell envelope. J Biol Chem 294:14175–14184. https://doi.org/10.1074/jbc.AW119.008139.
21. Malinverni JC, Silhavy TJ. 2009. An ABC transport system that maintains lipid asymmetry in the gram-negative outer membrane. Proc Natl Acad Sci U S A 106:8009–8014. https://doi.org/10.1073/pnas.0903229106.
22. Tang X, Chang S, Qiao W, Luo Q, Chen Y, Jia Z, Coleman J, Zhang K, Wang T, Zhang Z, Zhang C, Zhu X, Wei X, Dong C, Zhang X, Dong H. 2021. Structural insights into outer membrane asymmetry maintenance in Gram-

negative bacteria by MlaFEDB. Nat Struct Mol Biol 28:81–91. https://doi.org/10.1038/s41594-020-00532-y.
23. May KL, Silhavy TJ. 2018. The *Escherichia coli* phospholipase PldA regulates outer membrane homeostasis via lipid signaling. mBio 9:e00718-18. https://doi.org/10.1128/mBio.00718-18.
24. Mitchell AM, Wang W, Silhavy TJ. 2017. Novel RpoS-dependent mechanisms strengthen the envelope permeability barrier during stationary phase. J Bacteriol 199:e00708-16. https://doi.org/10.1128/JB.00708-16.
25. Mitchell AM, Srikumar T, Silhavy TJ. 2018. Cyclic enterobacterial common antigen maintains the outer membrane permeability barrier of *Escherichia coli* in a manner controlled by YhdP. mBio 9:e01321-18. https://doi.org/10.1128/mBio.01321-18.
26. Finn RD, Mistry J, Schuster-Bockler B, Griffiths-Jones S, Hollich V, Lassmann T, Moxon S, Marshall M, Khanna A, Durbin R, Eddy SR, Sonnhammer EL, Bateman A. 2006. Pfam: clans, web tools and services. Nucleic Acids Res 34:D247–D251. https://doi.org/10.1093/nar/gkj149.
27. Levine TP. 2019. Remote homology searches identify bacterial homologues of eukaryotic lipid transfer proteins, including Chorein-N domains in TamB and AsmA and Mdm31p. BMC Mol Cell Biol 20:43. https://doi.org/10.1186/s12860-019-0226-z.
28. Stubenrauch CJ, Lithgow T. 2019. The TAM: a translocation and assembly module of the beta-barrel assembly machinery in bacterial outer membranes. EcoSal Plus https://doi.org/10.1128/ecosalplus.ESP-0036-2018.
29. Josts I, Stubenrauch CJ, Vadlamani G, Mosbahi K, Walker D, Lithgow T, Grinter R. 2017. The structure of a conserved domain of TamB reveals a hydrophobic beta taco fold. Structure 25:1898–1906. https://doi.org/10.1016/j.str.2017.10.002.
30. Lees JA, Reinisch KM. 2020. Inter-organelle lipid transfer: a channel model for Vps13 and chorein-N motif proteins. Curr Opin Cell Biol 65:66–71. https://doi.org/10.1016/j.ceb.2020.02.008.
31. Heinz E, Selkrig J, Belousoff MJ, Lithgow T. 2015. Evolution of the translocation and assembly module (TAM). Genome Biol Evol 7:1628–1643. https://doi.org/10.1093/gbe/evv097.
32. Jumper J, Evans R, Pritzel A, Green T, Figurnov M, Ronneberger O, Tunyasuvunakool K, Bates R, Zidek A, Potapenko A, Bridgland A, Meyer C, Kohl SAA, Ballard AJ, Cowie A, Romera-Paredes B, Nikolov S, Jain R, Adler J, Back T, Petersen S, Reiman D, Clancy E, Zielinski M, Steinegger M, Pacholska M, Berghammer T, Bodenstein S, Silver D, Vinyals O, Senior AW, Kavukcuoglu K, Kohli P, Hassabis D. 2021. Highly accurate protein structure prediction with AlphaFold. Nature 596:583–589. https://doi.org/10.1038/s41586-021-03819-2.
33. Osawa T, Kotani T, Kawaoka T, Hirata E, Suzuki K, Nakatogawa H, Ohsumi Y, Noda NN. 2019. Atg2 mediates direct lipid transfer between membranes for autophagosome formation. Nat Struct Mol Biol 26:281–288. https://doi.org/10.1038/s41594-019-0203-4.
34. Otomo T, Maeda S. 2019. ATG2A transfers lipids between membranes *in vitro*. Autophagy 15:2031–2032. https://doi.org/10.1080/15548627.2019.1659622.
35. Valverde DP, Yu S, Boggavarapu V, Kumar N, Lees JA, Walz T, Reinisch KM, Melia TJ. 2019. ATG2 transports lipids to promote autophagosome biogenesis. J Cell Biol 218:1787–1798. https://doi.org/10.1083/jcb.201811139.
36. Ruiz N, Falcone B, Kahne D, Silhavy TJ. 2005. Chemical conditionality: a genetic strategy to probe organelle assembly. Cell 121:307–317. https://doi.org/10.1016/j.cell.2005.02.014.
37. Deng M, Misra R. 1996. Examination of AsmA and its effect on the assembly of *Escherichia coli* outer membrane proteins. Mol Microbiol 21:605–612. https://doi.org/10.1111/j.1365-2958.1996.tb02568.x.
38. Iqbal H, Kenedy MR, Lybecker M, Akins DR. 2016. The TamB ortholog of Borrelia burgdorferi interacts with the beta-barrel assembly machine (BAM) complex protein BamA. Mol Microbiol 102:757–774. https://doi.org/10.1111/mmi.13492.
39. Smith KP, Voogt RD, Ruiz T, Mintz KP. 2016. The conserved carboxyl domain of MorC, an inner membrane protein of *Aggregatibacter actinomycetemcomitans*, is essential for membrane function. Mol Oral Microbiol 31:43–58. https://doi.org/10.1111/omi.12120.
40. Misra R, Miao Y. 1995. Molecular analysis of *asmA*, a locus identified as the suppressor of OmpF assembly mutants of *Escherichia coli* K-12. Mol Microbiol 16:779–788. https://doi.org/10.1111/j.1365-2958.1995.tb02439.x.
41. Xiong X, Deeter JN, Misra R. 1996. Assembly-defective OmpC mutants of Escherichia coli K-12. J Bacteriol 178:1213–1215. https://doi.org/10.1128/jb.178.4.1213-1215.1996.
42. Selkrig J, Mosbahi K, Webb CT, Belousoff MJ, Perry AJ, Wells TJ, Morris F, Leyton DL, Totsika M, Phan MD, Celik N, Kelly M, Oates C, Hartland EL, Robins-Browne RM, Ramarathinam SH, Purcell AW, Schembri MA, Strugnell RA, Henderson IR, Walker D, Lithgow T. 2012. Discovery of an archetypal protein transport system in bacterial outer membranes. Nat Struct Mol Biol 19:506–510. https://doi.org/10.1038/nsmb.2261.
43. Wu T, Malinverni J, Ruiz N, Kim S, Silhavy TJ, Kahne D. 2005. Identification of a multicomponent complex required for outer membrane biogenesis in *Escherichia coli*. Cell 121:235–245. https://doi.org/10.1016/j.cell.2005.02.015.
44. Gruss F, Zahringer F, Jakob RP, Burmann BM, Hiller S, Maier T. 2013. The structural basis of autotransporter translocation by TamA. Nat Struct Mol Biol 20:1318–1320. https://doi.org/10.1038/nsmb.2689.
45. Bialer MG, Ruiz-Ranwez V, Sycz G, Estein SM, Russo DM, Altabe S, Sieira R, Zorreguieta A. 2019. MapB, the *Brucella suis* TamB homologue, is involved in cell envelope biogenesis, cell division and virulence. Sci Rep 9:2158. https://doi.org/10.1038/s41598-018-37668-3.
46. Stubenrauch C, Belousoff MJ, Hay ID, Shen HH, Lillington J, Tuck KL, Peters KM, Phan MD, Lo AW, Schembri MA, Strugnell RA, Waksman G, Lithgow T. 2016. Effective assembly of fimbriae in *Escherichia coli* depends on the translocation assembly module nanomachine. Nat Microbiol 1:16064. https://doi.org/10.1038/nmicrobiol.2016.64.
47. Azari F, Nyland L, Yu C, Radermacher M, Mintz KP, Ruiz T. 2013. Ultrastructural analysis of the rugose cell envelope of a member of the Pasteurellaceae family. J Bacteriol 195:1680–1688. https://doi.org/10.1128/JB.02149-12.
48. Gallant CV, Sedic M, Chicoine EA, Ruiz T, Mintz KP. 2008. Membrane morphology and leukotoxin secretion are associated with a novel membrane protein of *Aggregatibacter actinomycetemcomitans*. J Bacteriol 190:5972–5980. https://doi.org/10.1128/JB.00548-08.
49. Yu J, Li T, Dai S, Weng Y, Li J, Li Q, Xu H, Hua Y, Tian B. 2017. A tamB homolog is involved in maintenance of cell envelope integrity and stress resistance of Deinococcus radiodurans. Sci Rep 7:45929. https://doi.org/10.1038/srep45929.
50. Bernstein HD. 2019. Type V secretion in Gram-negative bacteria. EcoSal Plus https://doi.org/10.1128/ecosalplus.ESP-0031-2018.
51. Ruiz N. 2008. Bioinformatics identification of MurJ (MviN) as the peptidoglycan lipid II flippase in *Escherichia coli*. Proc Natl Acad Sci U S A 105:15553–15557. https://doi.org/10.1073/pnas.0808352105.
52. Wall E, Majdalani N, Gottesman S. 2018. The complex Rcs regulatory cascade. Annu Rev Microbiol 72:111–139. https://doi.org/10.1146/annurev-micro-090817-062640.
53. Whitfield C, Wear SS, Sande C. 2020. Assembly of bacterial capsular polysaccharides and exopolysaccharides. Annu Rev Microbiol 74:521–543. https://doi.org/10.1146/annurev-micro-011420-075607.
54. Jorgenson MA, Kannan S, Laubacher ME, Young KD. 2016. Dead-end intermediates in the enterobacterial common antigen pathway induce morphological defects in *Escherichia coli* by competing for undecaprenyl phosphate. Mol Microbiol 100:1–14. https://doi.org/10.1111/mmi.13284.
55. Jorgenson MA, Young KD. 2016. Interrupting biosynthesis of O antigen or the lipopolysaccharide core produces morphological defects in *Escherichia coli* by sequestering undecaprenyl phosphate. J Bacteriol 198:3070–3079. https://doi.org/10.1128/JB.00550-16.
56. Hews CL, Cho T, Rowley G, Raivio TL. 2019. Maintaining integrity under stress: envelope stress response regulation of pathogenesis in Gram-negative bacteria. Front Cell Infect Microbiol 9:313. https://doi.org/10.3389/fcimb.2019.00313.
57. Lima S, Guo MS, Chaba R, Gross CA, Sauer RT. 2013. Dual molecular signals mediate the bacterial response to outer-membrane stress. Science 340:837–841. https://doi.org/10.1126/science.1235358.
58. Konovalova A, Kahne DE, Silhavy TJ. 2017. Outer membrane biogenesis. Annu Rev Microbiol 71:539–556. https://doi.org/10.1146/annurev-micro-090816-093754.
59. Grabowicz M. 2019. Lipoproteins and their trafficking to the outer membrane. EcoSal Plus 8. https://doi.org/10.1128/ecosalplus.ESP-0038-2018.
60. Malinverni J, Werner J, Kim S, Sklar JG, Kahne D, Misra R, Silhavy TJ. 2006. YfiO stabilizes the YaeT complex and is essential for outer membrane protein assembly in *Escherichia coli*. Mol Microbiol 61:151–164. https://doi.org/10.1111/j.1365-2958.2006.05211.x.
61. Leive L. 1965. Release of lipopolysaccharide by EDTA treatment of *E. coli*. Biochem Biophys Res Commun 21:290–296. https://doi.org/10.1016/0006-291x(65)90191-9.
62. Guzman LM, Belin D, Carson MJ, Beckwith J. 1995. Tight regulation, modulation, and high-level expression by vectors containing the arabinose PBAD promoter. J Bacteriol 177:4121–4130. https://doi.org/10.1128/jb.177.14.4121-4130.1995.
63. Kumar N, Leonzino M, Hancock-Cerutti W, Horenkamp FA, Li P, Lees JA, Wheeler H, Reinisch KM, De Camilli P. 2018. VPS13A and VPS13C are lipid

transport proteins differentially localized at ER contact sites. J Cell Biol 217:3625–3639. https://doi.org/10.1083/jcb.201807019.
64. Dziurdzik SK, Conibear E. 2021. The Vps13 family of lipid transporters and its role at membrane contact sites. Int J Mol Sci 22:2905. https://doi.org/10.3390/ijms22062905.
65. Ugur B, Hancock-Cerutti W, Leonzino M, De Camilli P. 2020. Role of VPS13, a protein with similarity to ATG2, in physiology and disease. Curr Opin Genet Dev 65:61–68. https://doi.org/10.1016/j.gde.2020.05.027.
66. Jones NC, Osborn MJ. 1977. Translocation of phospholipids between the outer and inner membranes of *Salmonella typhimurium*. J Biol Chem 252:7405–7412. https://doi.org/10.1016/S0021-9258(19)66979-6.
67. Langley KE, Hawrot E, Kennedy EP. 1982. Membrane assembly: movement of phosphatidylserine between the cytoplasmic and outer membranes of *Escherichia coli*. J Bacteriol 152:1033–1041. https://doi.org/10.1128/jb.152.3.1033-1041.1982.
68. Li P, Lees JA, Lusk CP, Reinisch KM. 2020. Cryo-EM reconstruction of a VPS13 fragment reveals a long groove to channel lipids between membranes. J Cell Biol 219:e202001161. https://doi.org/10.1083/jcb.202001161.
69. Tran AX, Dong C, Whitfield C. 2010. Structure and functional analysis of LptC, a conserved membrane protein involved in the lipopolysaccharide export pathway in *Escherichia coli*. J Biol Chem 285:33529–33539. https://doi.org/10.1074/jbc.M110.144709.
70. Suits MD, Sperandeo P, Deho G, Polissi A, Jia Z. 2008. Novel structure of the conserved gram-negative lipopolysaccharide transport protein A and mutagenesis analysis. J Mol Biol 380:476–488. https://doi.org/10.1016/j.jmb.2008.04.045.
71. Bayer ME. 1968. Areas of adhesion between wall and membrane of *Escherichia coli*. J Gen Microbiol 53:395–404. https://doi.org/10.1099/00221287-53-3-395.
72. Cian MB, Giordano NP, Masilamani R, Minor KE, Dalebroux ZD. 2019. *Salmonella enterica* serovar Typhimurium uses PbgA/YejM to regulate lipopolysaccharide assembly during bacteremia. Infect Immun 88:e00758-19. https://doi.org/10.1128/IAI.00758-19.
73. Fivenson EM, Bernhardt TG. 2020. An essential membrane protein modulates the proteolysis of LpxC to control lipopolysaccharide synthesis in *Escherichia coli*. mBio 11:e00939-20. https://doi.org/10.1128/mBio.00939-20.
74. Guest RL, Same Guerra D, Wissler M, Grimm J, Silhavy TJ. 2020. YejM modulates activity of the YciM/FtsH protease complex to prevent lethal accumulation of lipopolysaccharide. mBio 11:e00598-20. https://doi.org/10.1128/mBio.00598-20.
75. Lutkenhaus J. 2020. Asymmetry is the rhythmic expression of functional design, a quotation from Jan Tschichold. J Bacteriol 202. https://doi.org/10.1128/JB.00370-20.
76. Nguyen D, Kelly K, Qiu N, Misra R. 2020. YejM controls LpxC levels by regulating protease activity of the FtsH/YciM complex of *Escherichia coli*. J Bacteriol 202:e00303-20. https://doi.org/10.1128/JB.00303-20.
77. Simpson BW, Douglass MV, Trent MS. 2020. Restoring balance to the outer membrane: YejM's role in LPS regulation. mBio 11:e02624-20. https://doi.org/10.1128/mBio.02624-20.
78. Blattner FR, Plunkett G, III, Bloch CA, Perna NT, Burland V, Riley M, Collado-Vides J, Glasner JD, Rode CK, Mayhew GF, Gregor J, Davis NW, Kirkpatrick HA, Goeden MA, Rose DJ, Mau B, Shao Y. 1997. The complete genome sequence of *Escherichia coli* K-12. Science 277:1453–1462. https://doi.org/10.1126/science.277.5331.1453.
79. Baba T, Ara T, Hasegawa M, Takai Y, Okumura Y, Baba M, Datsenko KA, Tomita M, Wanner BL, Mori H. 2006. Construction of *Escherichia coli* K-12 in-frame, single-gene knockout mutants: the Keio collection. Mol Syst Biol 2:2006.0008. https://doi.org/10.1038/msb4100050.
80. Silhavy TJ, Berman ML, Enquist LW. 1984. Experiments with gene fusions. Cold Spring Harbor Laboratory, Cold Spring Harbor, NY.
81. Cherepanov PP, Wackernagel W. 1995. Gene disruption in *Escherichia coli*: tcR and KmR cassettes with the option of Flp-catalyzed excision of the antibiotic-resistance determinant. Gene 158:9–14. https://doi.org/10.1016/0378-1119(95)00193-a.
82. Datsenko KA, Wanner BL. 2000. One-step inactivation of chromosomal genes in *Escherichia coli* K-12 using PCR products. Proc Natl Acad Sci U S A 97:6640–6645. https://doi.org/10.1073/pnas.120163297.
83. Yu D, Ellis HM, Lee EC, Jenkins NA, Copeland NG, Court DL. 2000. An efficient recombination system for chromosome engineering in *Escherichia coli*. Proc Natl Acad Sci U S A 97:5978–5983. https://doi.org/10.1073/pnas.100127597.
84. Ruiz N, Wu T, Kahne D, Silhavy TJ. 2006. Probing the barrier function of the outer membrane with chemical conditionality. ACS Chem Biol 1:385–395. https://doi.org/10.1021/cb600128v.
85. Vischer NO, Verheul J, Postma M, van den Berg van Saparoea B, Galli E, Natale P, Gerdes K, Luirink J, Vollmer W, Vicente M, den Blaauwen T. 2015. Cell age dependent concentration of *Escherichia coli* divisome proteins analyzed with ImageJ and ObjectJ. Front Microbiol 6:586. https://doi.org/10.3389/fmicb.2015.00586.
86. Ashkenazy H, Abadi S, Martz E, Chay O, Mayrose I, Pupko T, Ben-Tal N. 2016. ConSurf 2016: an improved methodology to estimate and visualize evolutionary conservation in macromolecules. Nucleic Acids Res 44:W344–W350. https://doi.org/10.1093/nar/gkw408.